J|A|C|S
ARTICLES

Published on Web 07/13/2010

Ridge-Tile-like Chiral Topology: Synthesis, Resolution, and Complete Chiroptical Characterization of Enantiomers of Edge-Sharing Binuclear Square Planar Complexes of Ni(II) Bearing Achiral Ligands

Vadim A. Soloshonok,*[,†] Taizo Ono,[‡] Hisanori Ueki,[§] Nicolas Vanthuyne,[||] Teodor Silviu Balaban,[||,⊥] Jochen Bürck,[#] Heike Fliegl,[⊥] Wim Klopper,[⊥] Jean-Valère Naubron,[||] Tam T. T. Bui,[▽] Alex F. Drake,[▽] and Christian Roussel*[,||]

Institute of Biorganic Chemistry and Petrochemistry, National Academy of Sciences of the Ukraine, Murmanska Street 1, Kyiv-94 02660, Ukraine, National Institute of Advanced Industrial Science and Technology, Nagoya, Japan, National Institute for Materials Sciences, Tsukuba, Japan, Chirosciences, ISM2, Université Paul Cézanne Aix-Marseille III, Case A62 Avenue Escadrille Normandie-Niemen, 13397 Marseille CEDEX 20, France, Institut für Nanotechnologie and Center for Functional Nanostrutures at the Karlsruhe Institute of Technology, Karlsruhe, Germany, Institut für Biologische Grenzflächen, Karlsruhe Institute of Technology, Karlsruhe, Germany, and Biomolecular Spectroscopy Centre, King's College London, The Wolfson Wing, Hodgkin Building, Guy's Campus, London SE1 1UL, United Kingdom

Received April 19, 2010; E-mail: christian.roussel@univ-cezanne.fr; vadimsoloshonok@gmail.com

Abstract: Binuclear square planar Ni(II) complexes are described, formed by two tridentate ligands with two imine-nitrogens coordinating two nickel atoms. Such complexes are synthetically readily available with great structural variety and present new types of ridge-tile-like chiral compounds that are reasonably stable in the appropriate "bent" conformation. Enantiomerically pure samples of these compounds have been obtained for the first time using HPLC with a chiral stationary phase. Absolute configurations and chiroptical properties are fully characterized by ECD, VCD, ORD spectroscopy, and theoretical calculations. These new compounds with ridge-tile-like chiral topology are configurationally reasonably stable [$\Delta G^{\ddagger} = 121.4$ kJ mol^{-1}, $t_{1/2} = 14.9$ h (78 °C, ethanol)], and therefore their chemistry, physical properties, and applications can be systematically studied.

Introduction

A bent conformation adopted by two adjacent square planar coordinated M(II) atoms and the appropriate arrangement of achiral ligands can lead to chiral objects. As illustrated in Figure 1, when the two M(II) metals are the same and the two connecting ligands X are identical, an inventory based upon achiral and chiral topologies can be drawn up of the stereochemical situations that may be encountered depending on the nature of the four remaining achiral ligands (A, B, C, and D).

When A ≠ B ≠ C ≠ D, chiral objects are obtained whatever the combination or location of the four achiral ligands. In the case A ≠ B ≠ C = D ≡ A ≠ B ≠ C2, there are three possible chiral arrangements. For A = B ≠ C = D ≡ A2 ≠ C2, two of the three possible arrangements are achiral and one is chiral. For A ≠ B = C = D ≡ A ≠ C3, the single arrangement is chiral. Finally, when the four ligands are identical, the complex is achiral. Note the achiral compounds in Figure 1 contain a mirror plane running through the edge-sharing axis and/or the two metal centers. If the two metals or the connecting ligands (X, X) were different, many more possibilities would be

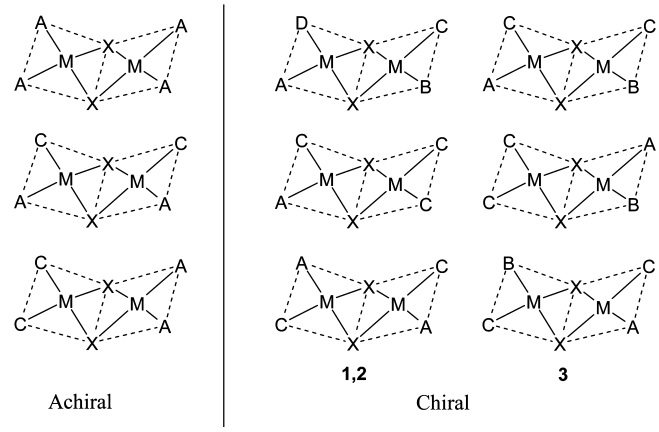

Figure 1. Achiral and chiral topologies resulting from bent edge-sharing binuclear square planar complexes of a d^8 transition metal when both two metals and the edge ligands are identical and the four remaining ligands A, B, C, and D are achiral. **1**, **2**, and **3** refer to the class of compounds synthesized and described in the present study.

[†] National Academy of Sciences of the Ukraine.
[‡] National Institute of Advanced Industrial Science and Technology.
[§] National Institute for Materials Sciences.
[||] Université Paul Cézanne Aix-Marseille III.
[⊥] Institut für Nanotechnologie and Center for Functional Nanostrutures at the Karlsruhe Institute of Technology.
[#] Karlsruhe Institute of Technology.
[▽] King's College London.

Scheme 1. Edge-Sharing Square Planar Binuclear Complexes of Ni(II) Bearing Achiral Ligands: **1**, **2**, and **3** (Bn = Benzyl)[a]

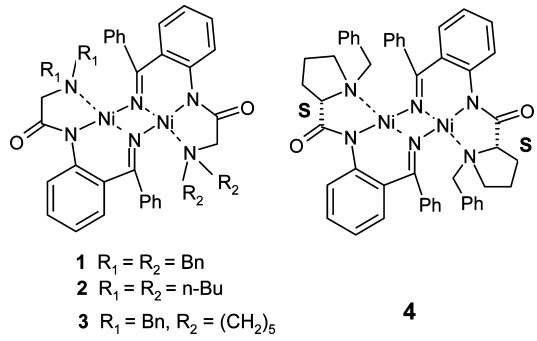

[a] Compound **4** presents additional chirality from the proline-based chiral ligands.

obtained, leading to a very attractive but as yet unexplored chirality domain.

The "ridge-tile-like" or "roof-type" complexes belong to the known class of edge-sharing binuclear square planar complexes of d^8 transition metal ions.[1] However, the chirality of this type of compound has been virtually ignored because the chiral bent conformation has been said to be highly unstable,[2] undergoing rapid inversion, similar to the chirality of trisubstituted nitrogen. To the best of our knowledge, there are no reported examples of the isolation and chiroptical characterization of the enantiomers of this type of chiral compound when the metals bear achiral ligands.

Here, the first description is reported of the synthesis, isolation, and full chiroptical characterization of the enantiomers of two types of edge-sharing binuclear square planar complexes of nickel(II) with chirality provided solely by a stable bent conformation and a suitable arrangement of achiral ligands. Two types of metal complex are considered represented by the compounds **1**, **2**, and **3** indicated in Figure 1 and illustrated in Scheme 1.

In a preliminary communication,[3] compound **4** (Scheme 1), which possesses two optically pure (*S*)-proline derived ligands, was shown to lead to unequally populated and isolatable diastereomeric forms. These diastereomers are hereafter called minor-**4** and major-**4**.

The existence of the diastereomers was the first physical proof of the chirality introduced by the bent conformation of the binuclear square planar nickel(II) complex in addition to the configurationally stable chirality center of the proline ligands. However, some degree of epimerization of the diastereomeric derivatives **4** was observed during storage in the solid state or

Scheme 2. Preparation of the Racemic Compounds **2** (a), **1** and **3** (b)[a]

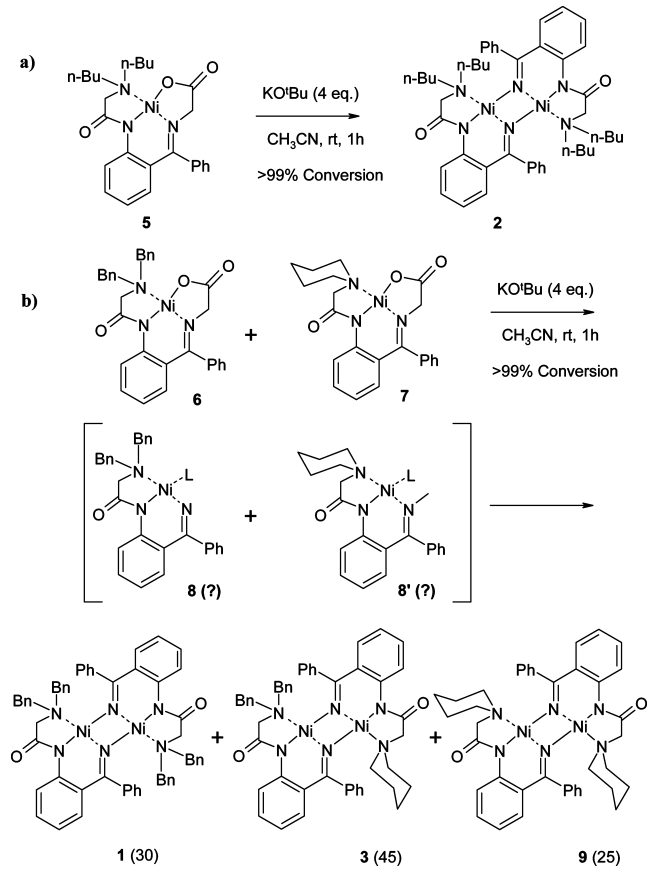

[a] Product proportions are given in parentheses.

in solution in various solvents. Doubt was cast on the stability of the edge-sharing configuration of the Ni(II) complexes of this type in general, compounds **1**, **2**, and **3** in particular, in which a higher flexibility of the less rigid ligands could be expected.

In this Article, the existence of chiral topologies resulting from bent edge-sharing binuclear square planar complexes of a d^8 transition metal has been unambiguous confirmed. The absolute configurations of the corresponding enantiomerically pure compounds have been assigned. These results pave the way to a systematic study of this fascinating and previously unexplored class of chiral structures.

Results and Discussion

Synthesis. The racemic compound **2** (Scheme 2a) was produced in a manner similar to the synthesis of the diastereomeric derivatives **4**.[3]

Exposure of a solution of the *n*-dibutylamine containing complex **5** in acetonitrile to the action of strong base resulted in quantitative formation of the binuclear product **2**, which was additionally purified by column chromatography (Scheme 2-a). The synthesis of compounds **1** and **3** was achieved by an interesting scrambling experiment. When a mixture of dibenzylamine **6** and piperidine **7** containing complexes was submitted to the same reaction conditions, the following three products were obtained: the corresponding dibenzylamine **1** and piperidine **9** derived dimers as expected, but also the scrambled product **3** (Scheme 2b). While detailed mechanistic rationale and the generality of this rare nitrogen reductive dealkylation

(1) (a) Aullón, G.; Ujaque, G.; Lledos, A.; Alvarez, S.; Alemany, P. *Inorg. Chem.* **1998**, *37*, 804–813. (b) Aullón, G.; Lledos, A.; Alvarez, S. *Inorg. Chem.* **2000**, *39*, 906–916. (c) Aullón, G.; Ujaque, G.; Lledos, A.; Alvarez, S. *Chem.-Eur. J.* **1999**, *5*, 1391–1410. (d) Marshall, W. J.; Aullón, G.; Alvarez, S.; Dobbs, K. D.; Grushin, V. V. *Eur. J. Inorg. Chem.* **2006**, 3340–3345. (e) Mizuta, T.; Aoki, S.; Nakayama, K.; Miyoshi, K. *Inorg. Chem.* **1999**, *38*, 4361–4364. (f) Aullón, G.; Alvarez, S. *Inorg. Chem.* **2001**, *40*, 4937–4946. (g) Lasri, J.; Kopylovich, M. N.; Guedes da Silva, M. F. C.; Charmier, M. A. J.; Pombeiro, A. J. L. *Chem.-Eur. J.* **2008**, *14*, 9312–9322. (h) Azerraf, C.; Cohen, S.; Gelman, D. *Inorg. Chem.* **2006**, *45*, 7010–7017.

(2) For examples of roof shape binuclear Ni complexes with additional chirality coming from chiral ligand, see: (a) Brunner, H.; Dormeier, S.; Grau, I.; Zabel, M. *Eur. J. Inorg. Chem.* **2002**, 2603–2613. (b) Duran, J.; Polo, A.; Real, J.; Benet-Buchholz, J.; Poater, A.; Sola, M. *Eur. J. Inorg. Chem.* **2003**, 4147–4151.

(3) Soloshonok, V. A.; Ueki, H. *J. Am. Chem. Soc.* **2007**, *129*, 2426–2427.

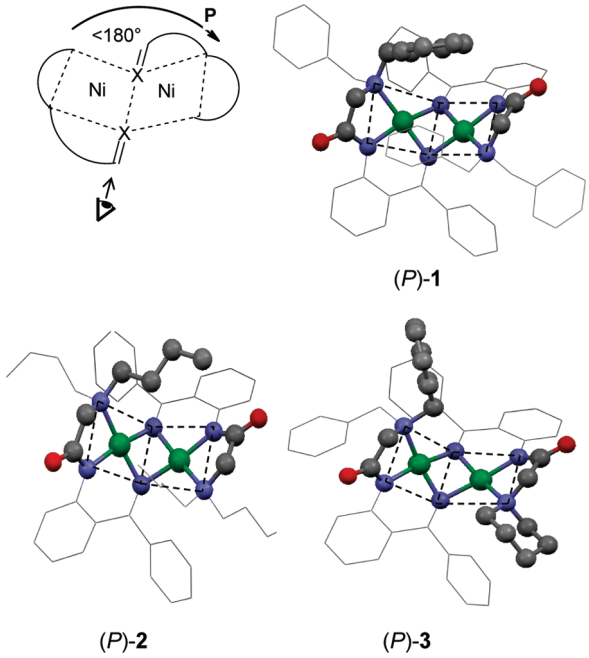

Figure 2. Absolute configuration nomenclature and selected enantiomer structures from the X-ray data of racemic **1**, **2**, and **3**. The dotted lines were added to highlight the roof-tile shape of the edge-sharing square planar binuclear complexes of Ni(II).

reaction still await more comprehensive studies, this result strongly supports the in situ formation of the intermediates **8** and **8′** (Scheme 2b), which can undergo further homo- or heterodimerization leading to symmetric or scrambled products.

The racemic products **1** and **3** were selected for this study and purified to analytical purity via column chromatography. The structures of compounds **1**, **2**, and **3** were confirmed by single crystal X-ray analysis.

Resolution of Enantiomers. The X-ray data of compounds **1**, **2**, and **3** showed that two enantiomers are observed in the solid state. While the X-ray data provide useful starting geometries of the enantiomers, which were used for further structure optimization, they do not shed light on the configurational stability of this type of chiral compound in solution. Figure 2 defines the absolute configuration nomenclature and illustrates the enantiomers (*P*)-**1**, (*P*)-**2**, and (*P*)-**3** as they appeared in the X-ray data. (Note: In the absence of established rules for the absolute stereochemistry nomenclature in this type of metal complex, it was now considered far more convenient and straightforward to use axial chirality with the chirality axis represented by the edge shared by the two square planar complexes. Unfortunately, this is an inverse nomenclature for the (*M*) and (*P*) forms as compared to the previous article, which was based upon helical chirality for the diastereomers of compound **4**. In the current Article and the Supporting Information, the X-ray structures of the assigned forms are reported to illustrate the absolute configuration without ambiguity.)

To study the unique chiroptical properties and assign the absolute configurations of the enantiomers with intact chirality, they need to be isolated. Provided the racemization of the isolated enantiomer is limited or nonexistent,[4,5] the method of choice for the enantiomer resolution of compounds **1**, **2**, and **3** is HPLC with chiral stationary phases (CSP). However, racemization can be a serious issue; a noticeable epimerization on storage has already been reported for **4**.[3]

The configurational stability of the enantiomers of **1**, **2**, and **3** is hopefully related to the strength of the coordination of the nickel with the nitrogen of the imine and/or the nickel with the nitrogen of the tertiary amine. The three structures under study and the diastereomeric pair **4** all include relatively basic tertiary amines. Therefore, the configurational stability should be high enough to permit a separation of the corresponding enantiomers using liquid chromatography with a chiral stationary phase.

Screening of various CSPs (see the Supporting Information) showed that the (*S*,*S*)-Whelk-O1 column from Regis was sufficiently efficient in separating the enantiomers of compounds **1**, **2**, and **3** as well as the diastereomers of **4** using a mobile phase composed of a mixture of hexane and an alcohol (EtOH or 2-PrOH): hexane/EtOH (1:1 v:v) for **1**, hexane/2-PrOH (8:2 v/v) for **2**, and pure EtOH for **3**. The peaks of the two enantiomers were consistently sharp with baseline separation yielding good resolution values: 2.55 for **1**, 4.52 for **2**, and 3.53 for **3**. The chromatograms did not show any plateau, a diagnostic for exchange between the enantiomers on the column.[6] The configurational stability of the enantiomers at room temperature was further confirmed during the check of their optical purity after semipreparative separation and careful evaporation of the solvent. Online CD detection at 390 nm showed that the first eluted enantiomers for compounds **1**, **2**, and **3** all gave a (+) CD_{390} sign. The CD_{390} sign of the first eluted diastereomer (less stable minor-**4**) of **4** is (−), indicative of a possible inversion of elution order between the diastereomers of **4** and the enantiomers of **1**, **2**, and **3** on the Whelk column. ECD and VCD spectrocopies (see below) prove that the first eluted diastereomer (less stable minor-**4**) of **4** has an opposite joining-edge absolute configuration to the first eluted enantiomers in the series **1**, **2**, **3**. These results show once again that liquid chromatography with chiral stationary phases is a very powerful method to separate enantiomers or diastereomers, but they also show that chiral HPLC cannot be used safely to assign the absolute configuration based upon elution order alone even on a given chiral stationary phase.[7] Semipreparative separations

(4) Piras, P.; Roussel, C. *J. Pharm. Biomed. Anal.* **2008**, *46*, 839–847.

(5) For some recent semi-preparative separations of metal complexes on chiral support, see: (a) Norel, L.; Rudolph, M.; Vanthuyne, N.; Williams, J. A. G.; Lescop, C.; Roussel, C.; Autschbach, J.; Crassous, J.; Reau, R. *Angew. Chem., Int. Ed.* **2010**, *49*, 99–102. (b) Setsune, J.-I.; Tsukajima, A.; Okasaki, N.; Lintuluoto, J. M.; Lintuluoto, M. *Angew. Chem., Int. Ed.* **2009**, *48*, 771–775. (c) Lai, R.; Chanon, F.; Roussel, C.; Sanz, M.; Vanthuyne, N.; Daran, J.-C. *J. Organomet. Chem.* **2008**, *693*, 23–32. (d) Rang, A.; Engeser, M.; Maier, N. M.; Nieger, M.; Lindner, W.; Schalley, C. A. *Chem.-Eur. J.* **2008**, *14*, 3855–3859. (e) Sun, P.; Krishnan, A.; Yadav, A.; Singh, S.; MacDonnell, F. M.; Armstrong, D. W. *Inorg. Chem.* **2007**, *46*, 10312–10320. (f) Warnke, M. M.; Cotton, F. A.; Armstrong, D. W. *Chirality* **2007**, *19*, 179–183. (g) Chen, X.; Okamoto, Y.; Yano, T.; Otsuki, J. *J. Sep. Sci.* **2007**, *30*, 713–716. (h) Lassen, P. R.; Guy, L.; Karame, I.; Roisnel, T.; Vanthuyne, N.; Roussel, C.; Cao, X.; Lombardi, R.; Crassous, J.; Freedman, T. B.; Nafie, L. A. *Inorg. Chem.* **2006**, *45*, 10230–10239. (i) Paisner, S. N.; Bergman, R. G. *J. Organomet. Chem.* **2001**, *621*, 242–245. (j) Ciclosi, M.; Lloret, J.; Estevan, F.; Lahuerta, P.; Sanau, M.; Pérez-Prieto, J. *Angew. Chem., Int. Ed.* **2006**, *45*, 6742–6744.

(6) For exchange processes on the chiral column, see: (a) Schurig, V. *J. Chromatogr., A* **2009**, *1216*, 1723–1736. (b) Wolf, C. *Chem. Soc. Rev.* **2005**, *34*, 595–608. (c) Trapp, O. *Anal. Chem.* **2006**, *78*, 189–198. (d) Trapp, O. *Chirality* **2006**, *18*, 489–497. (e) Vanthuyne, N.; Andreoli, F.; Fernandez, S.; Roman, M.; Roussel, C. *Lett. Org. Chem.* **2005**, *2*, 433–443. (f) Roussel, C.; Vanthuyne, N.; Bouchekara, M.; Djafri, A.; Elguero, J.; Alkorta, I. *J. Org. Chem.* **2008**, *73*, 403–411.

(7) Review: Roussel, C.; Del Rio, A.; Pierrot-Sanders, J.; Piras, P.; Vanthuyne, N. *J. Chromatogr., A* **2004**, *1037*, 311–3.

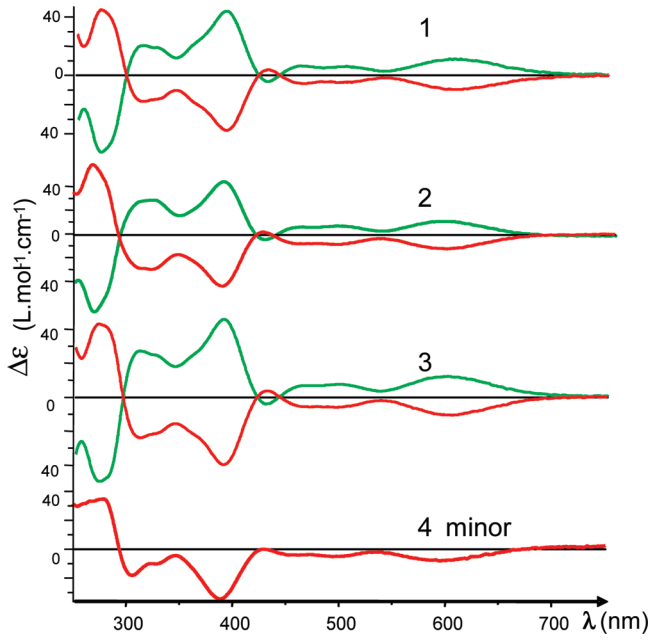

Figure 3. ECD spectra of the enantiomers of **1**−**3** (green, first eluted enantiomers; red, second eluted) and minor-**4** first eluted diastereomer (order of elution on the (*S*,*S*)-Whelk column, 2 mg/10 mL dry CH_2Cl_2).

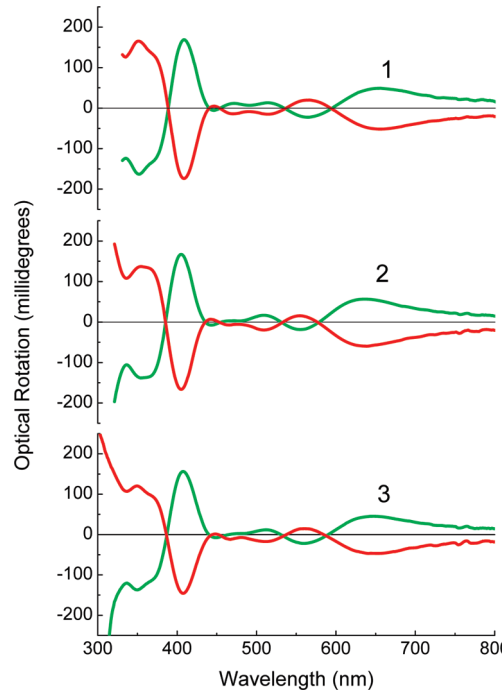

Figure 4. ORD spectra of the enantiomers of **1**−**3** in $CHCl_3$: green, first eluted enantiomers; red, second eluted (order of elution on the (*S*,*S*)-Whelk) column. Data were smoothed with a window factor of 8 for better presentation and normalized to $A_{390} = 1.0$.

of the enantiomers of compounds **1**, **2**, and **3** were successfully performed on the same chiral support, with resulting ee > 97%.

Chiroptical Properties of the Enantiomers of 1, 2, and 3. Electronic circular dichroism spectra (ECD) of the enantiomers of **1**, **2**, and **3** were recorded in dry CH_2Cl_2. The spectra are presented in Figure 3 together with the ECD spectra of the minor-**4** diastereomer.

The spectra are very similar showing that the substituent changes in the series **1**, **2**, and **3** do not affect the general shape of the ECD. Moreover, the CD intensities are almost identical for $\lambda > 350$ nm, some minor changes being observed for $\lambda <$ 350 nm. The ECD spectra of the enantiomers of **1**, **2**, and **3** are strikingly similar to those previously reported for the two isolated optically pure diastereomers of binuclear Ni(II) complexes **4** in which two additional stereogenic centers were introduced through two *N*-benzyl-(*S*)-proline residues.[3] The ECD spectra of the second eluted enantiomers of **1**, **2**, and **3** are strikingly similar to those of the first eluted minor diastereomer of **4** (minor-**4**) (red traces in Figure 3). The main contributions to the ECD spectra of the enantiomers of **1**−**3** and the diastereomers of **4** derive from the chiral core of the binuclear complex structure with only relatively minor contributions from the remote (chiral) substituents attached to the tertiary-amine.

The ORD curves, in the wavelength region 820−220 nm, for the enantiomers of **1**−**3** recorded in $CHCl_3$ are reported in Figure 4. Optical rotation is dependent on enantiomeric purity, concentration, and path length. To better ensure enantiomer comparison ensuring any variation is due only to enantiomeric purity, the ORD curves are reproduced here normalized to $A_{390} = 1.0$. A 10 mm cell path length was employed. The ORD curves of **1**, **2**, and **3** are very similar, and the spectra of the enantiomers effectively mirror each other. Again, the substituents on the tertiary amine have a relatively negligible effect on the chiroptical properties.

Enantiomers are frequently labeled as (+) or (−) based upon optical rotation data, normally at 589 nm. This is not trivial for the metal complexes described here. Absorption at 589 nm means a very low concentration would be required in the conventional 1.0 dm path length cell used in polarimetry to ensure that enough light is transmitted for detection. A positive CD maximum is observed near 589 nm. This will have an associated ORD bisignate Cotton effect with a zero (or close to zero) crossover at ~589 nm, giving at best a relatively low optical rotation. Throughout a series of compounds of this type, the crossover wavelength may vary, and hence sign will be uncertain. In this series of compounds, a considered wavelength needs to be chosen for the (+)/(−) nomenclature; $\lambda = 589$ nm is a bad choice. Reviewing the ORD spectra, we recommend that enantiomers are labeled according to the sign of their optical rotation at 365 nm, that is, $(+)_{365}$ or $(-)_{365}$, provided the concentration is extremely low. This should be readily measurable on a conventional polarimeter using a mercury lamp. Pathlengths shorter than 1 dm would be preferred. Even better would be recording optical rotation at 650 nm and labeling enantiomers as $(+)_{650}$ or $(-)_{650}$. The 650 nm optical rotation is relatively clear-cut and corresponds to the longest wavelength transition ORD Cotton effect maximum associated with the 590 nm CD. Unfortunately, this is not a measurement that could be made with a conventional polarimeter. It is worth noting that the sign of the optical rotation is opposite at 365 and 650 nm.

The great changes in optical rotation both in intensity and in sign with wavelength have practical issues when an online polarimeter is used to monitor chiral HPLC. For example, the observed sign using a JASCO OR-1590 online polarimeter detector results from the summation of contributions from several spectral components across the whole range of wavelengths from 350 to 900 nm in the mobile phase.[8] This technical issue has little consequence for the large majority of optically pure compounds, which present a simple ORD curve. However,

(8) Roussel, C.; Vanthuyne, N.; Serradeil-Albalat, M.; Vallejos, J.-C. *J. Chromatogr., A* **2003**, *995*, 79–85.

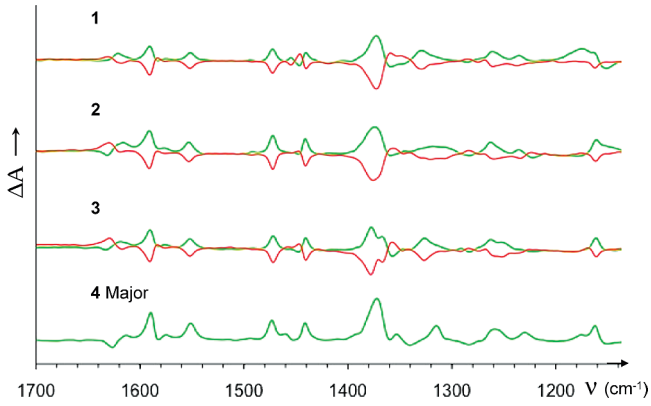

Figure 5. From top to bottom, experimental VCD spectra of **1**−**3** (green, first eluted enantiomers; red, second eluted) and major-**4** (second eluted) (lower TLC spot more stable, green). All spectra were recorded in CD_2Cl_2 with a concentration of 0.025 mol L^{-1} (order of elution on the (*S*,*S*)-Whelk column).

in the rare cases of multiple Cotton effects, as in this study, the optical rotation magnitude may be relatively weak due to sign cancellation, and the overall sign resulting from the summation over the whole range of wavelengths could be opposite to the one measured at 589 nm. The first eluted enantiomer for compounds **1**, **2**, and **3** gave a (−) sign according to JASCO OR-1590 online polarimeter. The observed sign could well be different using other commercially available online polarimeters, particularly those based upon single wavelength detection.

At this point of the discussion, according to ECD and ORD spectra, it can be safely stated that the second eluted enantiomers of complexes **1**, **2**, and **3** have the same absolute configuration at the edge-sharing binuclear Ni(II) square planar stereogenic element. This configuration is the same as the first eluted diastereomer of **4** (minor-**4**).

The VCD spectra of the enantiomers of **1**−**3** were recorded in CD_2Cl_2. Figure 5 shows that like the ECD and ORD, a consistent set of spectra are obtained across the series **1**−**3**. The VCD spectra of the major diastereomer of **4** (major-**4**, second eluted on the (*S*,*S*)-Whelk column) were also recorded and found to be similar to those obtained for the first eluted enantiomers of **1**−**3** (Figure 5, green curves).

As expected, the VCD spectra are more sensitive than ECD to substituent change on the tertiary amine. However, four bands situated at 1441, 1473, 1553, and 1591 cm^{-1} are excellent configuration markers. These VCD spectral components are all positive for the first eluted enantiomer in the series **1**−**3** and the second eluted enantiomer in major-**4**, confirming that they share the same absolute configuration at the binuclear Ni(II) complex fragment.

Absolute Configuration Determination. The assignment of absolute configuration was based upon calculated ECD and VCD spectra as compared to the experimental spectra. Compound **2** was selected for the calculations bearing in mind that relative configurations across the **1**, **2**, and **3** series are based upon ECD, ORD, and VCD spectra. Calculations of the predicted ECD and VCD spectra were performed on two fully optimized conformations of (*P*)-**2**: A-**2** (starting from the X-ray conformation) and B-**2** (C2-symmetry), which differ in the arrangement of the butyl groups (Figure 6). For the ECD spectra, all calculations were performed with the TURBOMOLE[9] program using density

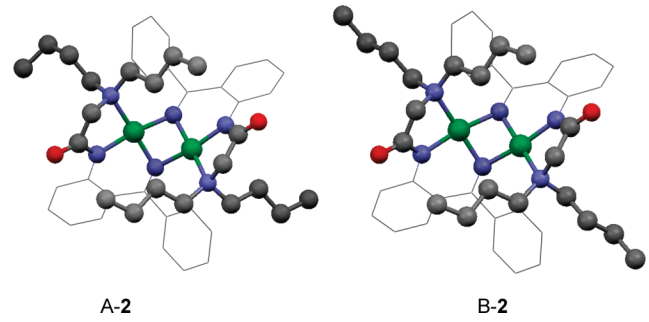

Figure 6. Display of two optimized conformations of (*P*)-**2**, which differ in the arrangement of the butyl groups.

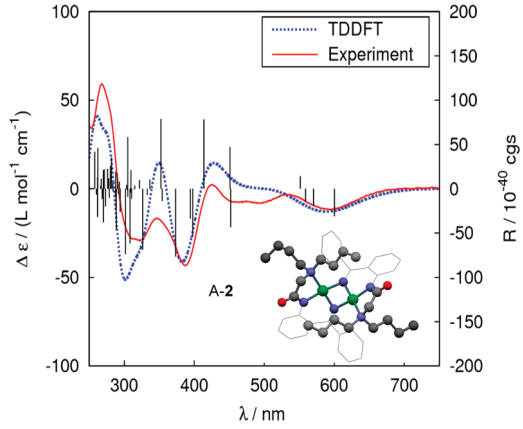

Figure 7. Comparison of experimental spectra (CH_2Cl_2) for second eluted **2** and calculated ECD spectra obtained for the optimized A-**2** conformation of (*P*)-**2**. The black bars correspond to calculated rotatory strengths.

functional theory (DFT). The B3LYP functional[10] was used together with the def2-SVP basis set.[11]

The ECD spectra were calculated for the two geometries A-**2** and B-**2** using time-dependent density functional theory (TD-DFT).[12] For all calculations, fine quadrature grids of size m4 were employed.[13] For a comparison between theoretical results and the experimental $\Delta\varepsilon$ values, the calculated ECD spectra have been modeled with Gaussian functions, using a root-mean-square width of 0.14 eV. It is worth noting that conformations A-**2** and B-**2** resulted in almost identical calculated ECD spectra. A clear assignment of the electronic transitions involved is difficult because the orbitals are not purely ligand or metal centered but delocalized over the phenyl ligands, the nitrogens, and the Ni atoms (see the Supporting Information). Bearing in mind that the calculations simulate the gas phase and that the calculated results have not been shifted, Figure 7 shows that the agreement between calculated and experimental spectra is relatively good, allowing a safe assignment of the absolute configuration.

(9) Ahlrichs, R.; Bär, M.; Horn, H.; Kölmel, C. *Chem. Phys. Lett.* **1989**, *162*, 165–169.

(10) (a) Slater, J. C. *Phys. Rev.* **1951**, *81*, 385–390. (b) Vosko, S. H.; Wilk, L.; Nusair, M. *Can. J. Phys.* **1980**, *58*, 1200–1211. (c) Lee, C.; Yang, W.; Parr, R. G. *Phys. Rev.* **1988**, *B37*, 785–789. (d) Becke, A. D. *Phys. Rev.* **1988**, *A38*, 3098–3100. (e) Becke, A. D. *J. Chem. Phys.* **1993**, *98*, 5648–5652. (f) Stephens, P. J.; Devlin, F. J.; Chablowski, C. F.; Frisch, M. J. *J. Phys. Chem.* **1994**, *98*, 11623–11627.

(11) Weigend, F.; Ahlrichs, R. *Phys. Chem. Chem. Phys.* **2005**, *7*, 3297–3305.

(12) (a) Furche, F.; Rappoport, D. Density functional methods for excited states: equilibrium structure and electronic spectra. In *Computational Photochemistry*; Olivucci, M., Ed.; Elsevier: Amsterdam, 2005; Vol. 16, Chapter III. (b) Bauernschmitt, R.; Ahlrichs, R. *Chem. Phys. Lett.* **1996**, *256*, 454–464.

(13) Treutler, O.; Ahlrichs, R. *J. Chem. Phys.* **1995**, *102*, 346–354.

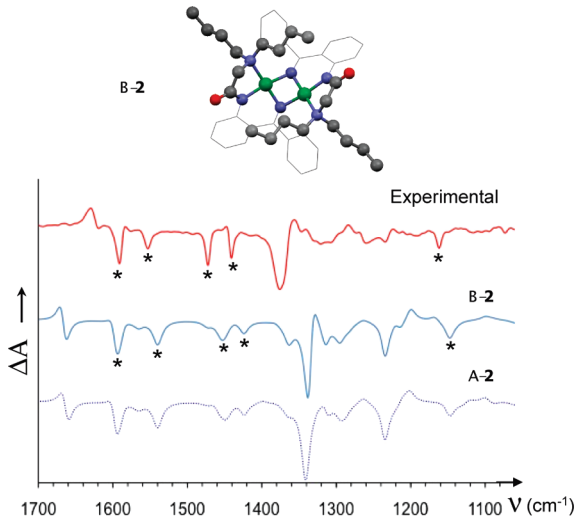

Figure 8. Comparison of experimental VCD spectra (CD_2Cl_2) for the second eluted **2** (in red) and calculated VCD spectra obtained for the optimized A-**2** and B-**2** conformation of (*P*)-**2**. The bands labeled with "*" are robust configuration markers (see text and the Supporting Information).

In conclusion, all of the (*S*,*S*)-Whelk second eluted enantiomers of compounds **1**−**3** present the same (*P*) absolute configuration depicted in Figure 2, and minor-**4** ((*S*,*S*)-Whelk first eluted) is (*P*,*S*,*S*).

For the VCD spectra, all calculations were performed using Gaussian software[14] to yield the optimized A-**2** and B-**2** conformations of (*P*)-**2**. Calculated VCDs were obtained using B3LYP functionals associated with the 6-31G(d,p) basis set for H, C, N, and O atoms. For Ni atoms, the MDF10 Stuttgart/Dresden ECP for core electrons and the associated basis set for valence electrons were used. Frequencies were scaled by a factor of 0.9627. The calculated VCD were very similar using A-**2** or B-**2** optimized geometries (Figure 8). In contrast to the ECD transitions in which the orbitals of Ni atoms were contributing, the calculated VCD frequencies in the range 1800−1000 cm^{-1} generally do not involve the Ni atoms except for the stretching of the Ni−N−C═O bonds at 1210 cm^{-1} (observed at 1223 cm^{-1}), which is mixed with the CH bending mode of the bridging phenyl groups. The four characteristic VCD bands are derived, respectively, from the antisymmetrical stretching of the two C═N bonds and the stretching of the C═C bond of the free phenyl moieties (calculated 1607 cm^{-1}, observed 1591 cm^{-1}), the antisymmetrical stretching of the C═C bond of the bridging phenyl moieties (calculated 1551 cm^{-1}, observed 1553 cm^{-1}), the stretching of the C═C bond of the bridging phenyl moieties with the CH_2 and CH_3 bending of the butyl groups (calculated 1460 cm^{-1}, observed 1473 cm^{-1}), and the rocking of the CH bonds of the phenyl moieties (calculated 1435 cm^{-1}, observed 1441 cm^{-1}). These bands are particularly well reproduced ("*" in Figure 8); they are negative for the second eluted enantiomers of **1**, **2**, and **3**. Analysis of the origin of these bands showed that they constitute a signature of the bridging phenyl groups and the imine ligands independently of the substituents on the tertiary amine and therefore observed in all of the enantiomers **1**−**3**, as well as in the corresponding proline diastereomers **4**. In the range of frequencies for which the VCD

(14) , Frisch, M. J.; et al. *Gaussian 03*, revision E.01; Gaussian, Inc.: Wallingford, CT, 2004.

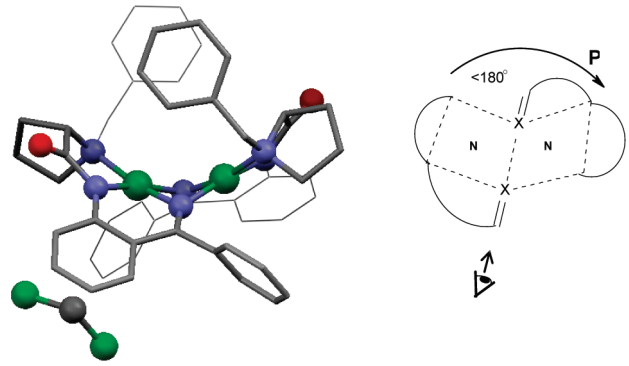

Figure 9. X-ray structure of the minor (*P*,*S*,*S*)-**4** showing the inclusion of CH_2Cl_2 in accordance with the experimental protocol.

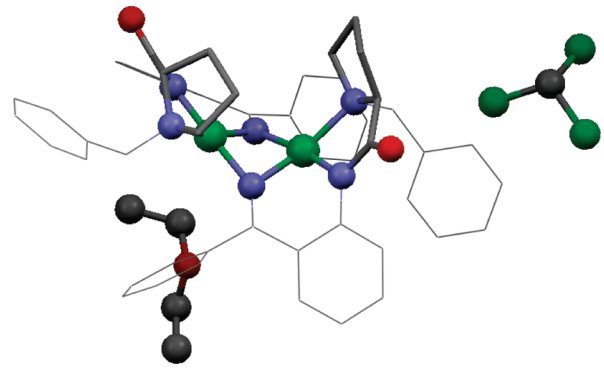

Figure 10. X-ray structure of the major (*M*,*S*,*S*)-**4** showing the inclusion of Et_2O and $CHCl_3$ in accordance with the experimental protocol.

was recorded, the Ni atoms are not directly involved. A good fit was observed between the experimental and calculated spectra (Figure 8).

The VCD study indicates that all of the second eluted enantiomers of compounds **1**−**3** present the same (*P*) absolute configuration depicted in Figure 8 and defined in Figure 2. The absolute configuration of the major-**4** second elution component is (*M*,*S*,*S*).

The absolute configurations of the diastereomers minor-**4** and major-**4** have been assigned by comparison of their ECD and VCD spectra with those predicted and observed for the pure enantiomers of **1**, **2**, and **3**. In the preliminary communication,[3] the Supporting Information records that the crystal of the minor diastereomer form of **4** (minor-**4**) used for X-ray crystallography was grown by a vapor diffusion method using CH_2Cl_2 and MeOH as solvents; the crystal of the major form (major-**4**) was grown by a vapor diffusion method using $CHCl_3$ and Et_2O as solvents. The X-ray structures of minor-**4** and major-**4** are reported in Figures 9 and 10; they are unambiguously identified thanks to the cocrystallization of CH_2Cl_2 with minor-**4** (Figure 9) and both $CHCl_3$ and Et_2O with major-**4** (Figure 10), respectively. The observed configurations are in perfect agreement with those derived from a comparison of ECD and VCD spectra.

Racemization. The minor (*P*,*S*,*S*)-**4** compound, after isolation, showed a tendency to give the major (*M*,*S*,*S*)-**4** compound on standing for weeks at room temperature. The qualitative observation of an epimerization process prompted a quantitative study of the configurational stability of the isolated enantiomers of **1**, **2**, and **3**. Ethanol at reflux was chosen as the solvent to follow the racemization kinetics. The enantiomers of **2** and **3** racemized very cleanly. Data analysis based upon a first-order

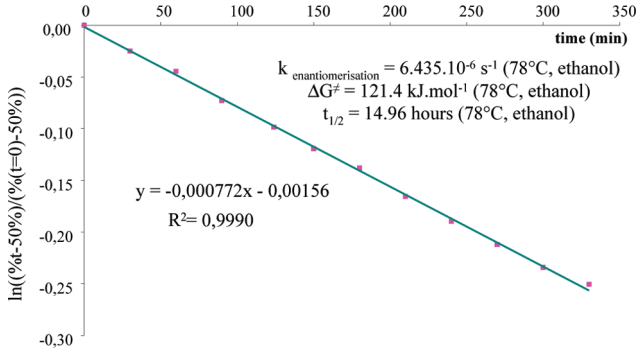

Figure 11. Enantiomerization kinetics of **2** in ethanol.

kinetic model gave a straight line from which the rate constant of enantiomerization can be extracted[15] (Figure 11). The participation of ethanol as a possible nickel ligand is not seen in these measurements because the ethanol is in very large excess, giving rise to pseudo first-order kinetics. The observed barriers of enantiomerization are almost identical for **2** and **3** ($\Delta G^{\ddagger} = 121.4$ kJ mol^{-1}, $t_{1/2} = 14.9$ h (78 °C, ethanol)).

For compound **1**, the estimated barrier is slightly higher than in **2** and **3**.[16] The required prolonged heating to achieve racemization of compound **1** results in extensive parallel chemical decomposition while refluxing in ethanol. A more systematic study of the solvent effect and of the role of the pK_a and steric bulk of the liganding amine on the barrier is in progress, and initial results show that these chiral compounds are not chemically inert.[17] However, the stability data do suggest that compounds **1**, **2**, and **3**, possessing the new ridge-tile-like chiral topology, are configurationally reasonably stable and therefore do offer new practical applications of this previously unstudied source of chirality.

(15) (a) Wolf, C. Racemization, enantiomerization and diastereomerization. *Dynamic Stereochemistry of Chiral Compounds, Principles and Applications*; RCS Publishing: Cambridge, UK, 2008; Chapter III. (b) Maskill, H. *The Physical Basis of Organic Chemistry*; Oxford University Press: Oxford, 1985.

(16) A barrier of 1 ($\Delta G^{\ddagger}$ = ca. 124 kJ mol^{-1}) was estimated from three available experimental points, which were perfectly aligned. This is not sufficient for a precise determination of the barrier; however, it provides evidence that the barrier is qualitatively higher in **1** than in **2** and **3**.

(17) In a very preliminary experiment, the replacement of the tertiary amine in **1**, **2**, or **3** by a less basic 2-carboxy-pyridine ligand results in a much lower barrier to racemization, giving rise to a plateau during room temperature chromatography on a chiral stationary phase (data not shown) and precluding isolation at room temperature of the enantiomers ($t_{1/2}$ = 11 min at 15 °C in EtOH). The tridendate nature of the ligand and the high basicity and steric bulk of the tertiary amine are the basis for the reasonable configurational stability observed in **1**, **2**, **3**, and **4**.

Conclusions

Chromatography with a chiral stationary phase has led to the first isolation of the enantiomers of two classes of stable "roof shape" bimetallic chiral complexes constructed around two nickel atoms. Off-line measurements of ECD and VCD spectra and associated DFT calculations on complex **2** have enabled an unambiguous assignment of the absolute configuration of the isolated enantiomers.[8] A remarkable similarity was observed in the ECD, ORD, and VCD spectra of the enantiomers of **1**−**3**. The second eluted enantiomers on the (*S*,*S*)-Whelk column of complexes **1**−**3**, which are characterized by a (+) sign using online JASCO polarimetric detection and a (−) sign using online CD detection at 390 nm, have a (*P*) absolute configuration. By comparison, the (*M*) absolute configuration is assigned to the first eluted enantiomers [(*S*,*S*)-Whelk column] of **1**−**3**, which are characterized by (+) CD signs at 390 and 590 nm, (−) sign using on-line JASCO polarimetric detection and optical rotations with $(-)_{365}$ and $(+)_{650}$.

Complexes **1**−**3** present the first examples of chirality due solely to the bent shape of the binuclear square planar Ni(II) complexes; there is no additional element of chirality brought by the ligands that are achiral. This new type of ridge-tile-like chiral topology has been demonstrated to be configurationally quite stable, opening a door for systematic studies and practical applications.

Acknowledgment. We thank the CRCMM and the Spectropôle Marseille for computer time and use of the VCD facility, respectively. The Deutsche Forschungsgemeinschaft is thanked for its support of the Center for Functional Nanostructures at the Karlsruhe Institute of Technology, which permitted the collaboration between the groups of Wim Klopper (theory), Anne Ulrich (CD Spectroscopy, project E1.2), and Silviu Balaban (project C3.5). A.F.D. and T.T.T.B. thank the Wellcome Foundation and Applied Photophysics for their support.

Supporting Information Available: Synthesis of **1**, **2**, **3**, and **4** (minor and major), chiral chromatography, optical rotation, ECD, IR, and VCD, Cartesian coordinates of conformations A-**2** and B-**2**, crystallographic information, kinetics of enantiomerization, and complete ref 14. This material is available free of charge via the Internet at http://pubs.acs.org.

JA103296G